Sub-seasonal Forecast Skill for Weekly Mean Atmospheric Variability over the Northern Hemisphere in Winter and its Relationship to Mid-Latitude Teleconnections

Akio Yamagami[1] and Mio Matsueda[2]

[1]University of Tsukuba
[2]University of Tsukuba & University of Oxford

November 26, 2022

Abstract

This study assesses the sub-seasonal predictability of the weekly mean geopotential height anomaly at 500 hPa and its relationship to teleconnections over the Northern Hemisphere in winter. The skill over the North Pacific, Canada, and Greenland is higher than over other areas for week-3 and -4 forecasts. These peaks correspond to the centers of action for the Pacific–North American (PNA) pattern and the North Atlantic Oscillation (NAO). PNA (NAO phase) predictions are better for El Niño years at lead times of 4 weeks (2–4 weeks). The effects of La Niña forcing on PNA and NAO forecasts are small compared with the El Niño forcing. Numerical models tend to predict a negative PNA at lead times of 3–4 weeks in La Niña years. The improvement in the mid-latitude upper-level jet rather than in the atmospheric response to ENSO forcing in the tropics is important for better S2S prediction.

Hosted file

`yamagami_matsueda_supplement_ver0.0.docx` available at https://authorea.com/users/381519/articles/606300-sub-seasonal-forecast-skill-for-weekly-mean-atmospheric-variability-over-the-northern-hemisphere-in-winter-and-its-relationship-to-mid-latitude-teleconnections

Sub-seasonal Forecast Skill for Weekly Mean Atmospheric Variability over the Northern Hemisphere in Winter and its Relationship to Mid-Latitude Teleconnections

Enter authors here: Akio Yamagami and Mio Matsueda

Center for Computational Sciences, University of Tsukuba, Japan.

Corresponding author: Akio Yamagami (yamagami@ccs.tsukuba.ac.jp)

Key Points:

- Mid-latitude teleconnections contribute to higher forecast skill over North Pacific, North America, and North Atlantic at S2S timescales.
- Forcing associated with El Niño can enhance the sub-seasonal predictability of mid-latitude teleconnections.
- Accurate prediction of the mid-latitude jet plays an important role in teleconnection forecasts at S2S timescales.

Abstract

This study assesses the sub-seasonal predictability of the weekly mean geopotential height anomaly at 500 hPa and its relationship to teleconnections over the Northern Hemisphere in winter. The skill over the North Pacific, Canada, and Greenland is higher than over other areas for week-3 and -4 forecasts. These peaks correspond to the centers of action for the Pacific–North American (PNA) pattern and the North Atlantic Oscillation (NAO). PNA (NAO phase) predictions are better for El Niño years at lead times of 4 weeks (2–4 weeks). The effects of La Niña forcing on PNA and NAO forecasts are small compared with the El Niño forcing. Numerical models tend to predict a negative PNA at lead times of 3–4 weeks in La Niña years. The improvement in the mid-latitude upper-level jet rather than in the atmospheric response to ENSO forcing in the tropics is important for better S2S prediction.

Plain Language Summary

Weather forecasts at medium-range timescales are basically skillful because of the evolution of numerical weather prediction systems. However, numerical models generally struggle to make accurate predictions at Sub-seasonal to seasonal (S2S; 2 week to 2 month range) timescales. Atmospheric low-frequency variability and atmosphere–ocean–land coupled processes are potential sources of improvements to S2S forecast skill. This study investigates the forecast skill of weekly mean atmospheric variability and its relationship to dominant teleconnections over the Northern Hemisphere in winter. The Sub-seasonal forecast skill (3–4 weeks) is higher over the North Pacific, Canada, and Greenland than over other areas. These regions correspond to the centers of action of the Pacific–North American (PNA) pattern and the North Atlantic Oscillation (NAO). Sub-seasonal forecasts of PNA and NAO are better in El Niño years than in neutral years. This indicates that ENSO conditions can enhance sub-seasonal predictability through improvements to PNA and NAO forecasts. In contrast, the numerical model used here tends to have a negative PNA bias in La Niña years. Both higher skill in certain regions and the negative PNA bias depend on the predictions of the upper-level jet in mid-latitudes. The upper-level jet predictions in mid-latitudes rather than the atmosphere-ocean coupling process predictions in tropics plays an important role in S2S timescales. Therefore, reducing the bias in mid-latitudes would improve the S2S forecasts.

1 Introduction

Sub-seasonal to seasonal (S2S) weather predictions have attracted increasing attention in recent years (Brunet et al., 2010). At medium-range timescales, forecast skill mainly depends on the initial atmospheric conditions (White et al., 2017). However, there are many contributions to predictability at S2S timescales. Atmosphere–ocean–land interactions (e.g., sea surface temperature, sea ice, snow cover, soil moisture) and atmospheric low-frequency variability (e.g., teleconnections and polar vortices) also affect forecast skill at S2S timescales.

The Pacific–North American (PNA) pattern is a dominant atmospheric teleconnection over the wintertime Northern Hemisphere (Wallace and Gutzlar, 1981). Atmospheric circulation associated with the PNA has a significant influence on the surface temperature and precipitation over North America (e.g., Yu et al., 2019). The North Atlantic Oscillation (NAO) is another dominant atmospheric variability (Walker and Bliss, 1932; Hurrell, 1995). The phase and strength of the NAO affect westerlies from the west coast of North America to Europe. Thus, the NAO has a significant impact on the weather of North America and western and central Europe. Although some studies have attributed the PNA to an internal atmospheric variability (e.g., Straus and Shukla, 2000, 2002), other studies have found that the El Niño–Southern Oscillation (ENSO) affects the PNA (and the Tropical–Northern Hemisphere pattern) through an extratropical response (e.g., Hoskins and Karoly, 1981; Soulard et al., 2019). In addition, the forcing associated with ENSO can modify the NAO phase (Zhang et al., 2015, 2019; Toniazzo and Scaife, 2006).

Extended-range ensemble predictions are conducted routinely by operational numerical weather prediction (NWP) centers around the world, and a database for such predictions was established by the S2S prediction project (Vitart et al., 2017). Many studies have focused on improvements to S2S prediction; e.g., forecast skills for Madden–Julian Oscillation (MJO) and its teleconnections (e.g., Tseng et al., 2017; Vitart, 2017), synoptic systems (e.g., Quinting and Vitart, 2019; Zheng et al. 2019), extreme events (e.g., DelSole et al., 2017; Lin, 2018; Wang and Robertson, 2019), and the sea ice edge (Zampieri et al., 2018, 2019) have been evaluated using this S2S dataset. Lin (2020) investigated the S2S forecast skill in the Northern polar region and showed that the skill depends on Arctic Oscillation and MJO phases. In this study, we investigate the forecast skill of operational S2S predictions for weekly mean atmospheric variability over the Northern Hemisphere. We focus on the relationship between spatial distribution of forecast skill and teleconnection patterns, particularly the PNA and NAO.

2 Data and Methods

2.1 *Data*

We used ensemble reforecast data from the S2S prediction project database (Vitart et al., 2017) from five NWP centers: Environmental and Climate Change Canada (ECCC), the European Centre for Medium-range Weather Forecasts (ECMWF), the Japan Meteorological Agency (JMA), the US National Centers for Environmental Prediction (NCEP), and the UK Met Office (UKMO). We only used reforecast data from ensemble prediction systems (EPSs) in operation in 2018. The configuration of each EPS is summarized in Table S1. The EPSs of the ECMWF, NCEP, and UKMO use a coupled atmosphere–ocean model, whereas those of the ECCC and JMA use an uncoupled model. One model version was used for all reforecast data of the JMA and NCEP EPSs, whereas several model updates were applied to the ECCC, ECMWF, and UKMO EPSs. Because data availability differs among the NWP centers, we used the ensemble reforecast data initialized each Thursday for the period 1999–2010 for all the EPSs. Therefore, the ECCC, ECMWF, and NCEP datasets have exactly the same initial dates, the number of which is greater than those of the JMA and UKMO datasets. These reforecast data have a grid spacing of 2.5° and a temporal resolution of 1 day.

The ECMWF Reanalysis (ERA)-5 data (Hersbach et al., 2019) were used to evaluate the reforecast data. The reanalysis data have the same grid spacing and temporal resolution as the forecast data.

2.2 *Weekly mean forecast skill*

The forecast skill was evaluated using the weekly mean geopotential height anomaly at 500 hPa (Z500 anomaly) in winter (December, January, and February; DJF). For ECCC, ECMWF, and NCEP, the week-1 forecast corresponds to the average of the first 7 forecast days, the week-2 forecast to forecast days 8 to 14, etc. When the 4th day of a weekly mean falls in DJF, we include the weekly mean in the analysis. For the JMA and UKMO, we regard the week-1 forecast as the period of the week-1 ECCC forecast beginning within a 3-day window centered on the initialization. For example, the week-1 UKMO forecast begins 9 Jan 1999 and extends 5 days to 14 Jan 1999, corresponding to the week-1 ECCC forecast initialized on 7 Jan 1999. Each model's climatology was estimated for each forecast lead time using reforecast data for 1995–2010 (1998–2010 for ECMWF and 1999–2010 for NCEP), within a 31-day time window centered on each initial day and a 7-day forecast time window centered on the forecast lead time of interest. The forecast skill was evaluated using the correlation between analyzed and predicted weekly mean Z500 anomalies at each grid point (i.e., "correlation skill" in Scaife et al. (2017)). Because of the small ensemble size of the reforecast, we focus on the skill of ensemble mean forecasts.

2.3 ENSO, PNA, and NAO indices

The ENSO conditions for each year were determined according to the seasonal Ocean Niño Index (ONI) obtained from the NOAA Climate Prediction Center webpage (https://origin.cpc.ncep.noaa.gov/products/analysis_monitoring/ensostuff/ONI_v5.php). We consider years with ONI ≥ 0.8 (ONI ≤ −0.8) in DJF as strong El Niño (La Niña) years.

The PNA index was calculated according to the pointwise definition of Wallace and Gutzler (1981). The Z500 anomaly is normalized by the climatological standard deviation (CSD) for each model. The CSD was estimated from the same reforecast dataset as used for the calculation of the model climatology at each lead time.

The NAO index was calculated by projecting the predicted Z500 anomaly in the region of (20°–90°N, 90°W–90°E) onto the first mode of the empirical orthogonal function (EOF) of the monthly mean Z500 anomaly from ERA5.

3 Results

3.1 Forecast skill over the Northern Hemisphere

The correlation skill over the Northern Hemisphere is greater than 0.6 for lead times of up to 2 weeks (not shown), but the skill drops rapidly over the Arctic and the Mediterranean Sea for lead times of 3 weeks (Fig. 1a–e). The skill is, however, ≥0.4 and significant at the 99% confidence level over the North Pacific, Canada to the south of Greenland, and Florida. Although the skill is almost zero over most regions of the Northern Hemisphere in the week-4 forecast, significant skill exists in these regions (except over Canada in the ECCC and JMA forecasts). These higher forecast skills compared with other areas are also evident in the week-5 ECMWF, NCEP (except over Canada), and UKMO forecasts. These results suggest that the weekly mean Z500 anomaly is predictable in certain mid- to high-latitude regions at S2S timescales. These regions correspond to the centers of action of the PNA and NAO. Therefore, we focus on the relationship between forecast skill and these teleconnections in subsequent sections.

3.2 Composite of the Z500 anomaly during El Niño and La Niña years

The composite Z500 anomaly calculated from the reanalysis during El Niño years (red panels in Fig. 2a and b) is positive over the Arctic, Kamchatka Peninsula, and Eastern Europe, and negative over the northeast Pacific and the North Atlantic. The anomaly corresponds to a positive PNA pattern over the North Pacific to North America and a negative NAO over the North Atlantic. During La Niña years, the anomaly calculated from the reanalysis is positive over the North Pacific (blue panels in Fig. 2c and d), the west coast of North America, and from the Kara Sea to eastern Europe, but negative over the Pacific side of the Arctic Ocean and China. Unlike El Niño years, the composite calculated from the reanalysis in La Niña years does not exhibit clear PNA or NAO patterns. The anomaly over North America is particularly small in the reanalysis. Note that the composites calculated from the reanalysis for JMA and UKMO are slightly different to those for ECCC, ECMWF, and NCEP (red and blue panels in Fig. 2) because of differences in the sample sizes used by each NWP center. However, these differences are much smaller than the differences between the composites of the analyzed and predicted anomalies.

The predicted anomaly during El Niño years is similar to the analyzed anomaly for all NWP centers for the week-1 and -2 forecasts, but with a weaker amplitude in the week-2 forecast (Fig. S1a and b). The week-3 forecasts from ECMWF and UKMO have composite patterns similar to the reanalysis, but those of ECCC, JMA, and NCEP are less similar to the reanalysis (see correlation coefficients in Fig. 2a). In particular, the positive anomaly over the Arctic and Canada is largely absent from the NCEP forecast. Although the anomaly weakens further in the week-4 forecasts (Fig. 2b), the week-3 and -4 forecasts, except for the 4-week JMA forecast, show a wave train over the North Pacific, Canada, and Florida, which corresponds to the positive PNA pattern. In addition, anomalies in the North Atlantic correspond to the negative NAO pattern in the week-3 forecasts, except for that from NCEP. As Scaife et al. (2014) showed, the UKMO model clearly predicts the negative NAO pattern even at a lead time of 4 weeks. The week-4 NCEP and UKMO forecasts show a higher correlation coefficient than the other NWP centers. These results suggest that the anomalies associated with the PNA and NAO were well predicted at S2S timescales during El Niño years by the NWP centers, but with a much smaller amplitude than that seen in the reanalysis.

During La Niña years, the positive anomaly over the North Pacific is well predicted at lead times up to 4 weeks by all NWP centers (Figs S1c–d and 2c–d). The negative anomaly over the Bering Strait is also well predicted up to lead times of 3 weeks, but the anomaly is stretched (shifted towards North America) in the ECCC and UKMO (ECMWF, JMA, and NCEP) forecasts. As a result, a negative PNA-like pattern is predicted at lead times of 3 and 4 weeks. This negative PNA-like pattern does not appear in the reanalysis. These results indicate that these NWP models tend to predict a negative PNA-like pattern in response to La Niña forcing at S2S timescales.

3.3 Forecast skill for PNA and NAO indices

The correlation skill and root-mean-square error (RMSE) between analyzed and predicted PNA indices are approximately 0.5 and 0.6, respectively, in the week-3 forecast (Table 1 and Fig. S2b). At this lead time, no consistent differences in PNA prediction exist between El Niño and neutral years among the NWP centers. The week-4 forecast for El Niño years has a higher correlation skill and a smaller RMSE than in neutral years for all NWP centers except UKMO. This result indicates that S2S predictability for PNA amplitude and phase is enhanced during El Niño years. The correlation skill (RMSE) is also higher (lower) for La Niña years than neutral years in the week-4 ECCC, ECMWF, and JMA forecasts, but is lower (higher) for La Niña years than neutral years in the week-4 NCEP and UKMO forecasts. That is, the forecasts generated by the NWP centers during La Niña years are inconsistent, even the week-4 forecasts.

Both the correlation skill and RMSE for the NAO forecasts were higher during El Niño years than neutral years for the week-2 -3, and -4 forecasts (Table 1 and Fig. S3). This suggests that the prediction of the NAO phase is more accurate during El Niño years than neutral years, but the predicted NAO amplitude is not. In contrast to the PNA index, the impact of El Niño forcing on the forecast skill for the NAO is evident after the week-2 forecasts. The week-4 UKMO forecast is of particularly high skill (≥0.6) in El Niño years. A larger increase in correlation skill is found for the ECMWF (0.56), NCEP (0.41), and UKMO (0.59) forecasts than for the ECCC (0.2) and JMA (0.1) forecasts for El Niño years in the week-4 forecasts. During La Niña years, the correlation skill of the NAO index is generally high compared with that of neutral years for all NWP centers up to a lead time of 4 weeks, except for the week-3 ECMWF and UKMO forecasts. The RMSE in La Niña years, however, is comparable to that in neutral years. These results indicate that the NAO phase is more predictable than the NAO amplitude for La Niña years.

3.4 Sea surface temperature (SST) anomaly and atmospheric response to ENSO forcing

One of the most significant differences in EPSs among NWP centers is the atmosphere–ocean coupling in the NWP model (Table S1). The composite SST anomaly calculated from the reanalysis is positive in the central Pacific during El Niño years (red shading in Fig. 3a, b). The positive anomaly is well represented in all NWP centers in the week-3 and -4 forecasts, although the anomaly extends farther into the eastern Pacific compared with that in the reanalysis. The negative anomaly of velocity potential (VP) in the upper troposphere associated with the positive SST anomaly is also predicted accurately by all NWP centers (contours in Fig. 3a, b). The differences in SST and VP anomalies in the tropics are small among the NWP centers, suggesting that the influence of the atmosphere–ocean coupling in the NWP model is small with respect to these processes. The differences in prediction among the NWP centers appear in the negative VP anomaly associated with the upper-level jet over the Northeast Pacific in week-4 (green hatching in Fig. 3b). For the ECMWF, NCEP, UKMO, and reanalysis, the upper-level jet continues from the North Pacific to North America, and a negative VP anomaly appears over the northeastern Pacific. In contrast, the Pacific jet over the Pacific separated from the Atlantic jet in the ECCC and JMA forecasts. The negative VP anomaly over the northeastern Pacific is small in these two forecasts compared with the other NWP centers and the reanalysis. The upper-level jet acts as a waveguide in the mid-latitudes (Hoskins and Ambrizzi, 1993), and this difference would be one of the reasons for the lower correlation skill over Canada in the week-4 ECCC and JMA forecasts (Fig. 1a and c).

During the La Niña years, the negative SST anomaly and convergent anomaly in the central Pacific are well represented by all of the NWP center forecasts (Fig. 3c, d). In the mid-latitudes, the exit of the Pacific jet is located around 140°W in the reanalysis. However, the predicted Pacific jet reaches the west coast of North America in all of the forecasts made by the NWP centers. The distribution of the predicted Pacific jet would enhance Rossby wave propagation. The predicted Pacific jet possibly leads to the negative PNA bias seen in the week-3 and -4 forecasts (Fig. 2c and d).

4 Summary and Conclusions

In this study, we used operational ensemble forecasts to assess the sub-seasonal predictability of the weekly mean Z500 anomaly and its relationship to teleconnections over the Northern Hemisphere in winter. In the week-3 and -4 forecasts, the skill over the North Pacific, Canada, and Greenland was higher than in other areas. The correlation skills over these regions were approximately 0.4, and were significant at the 99% confidence level. However, the correlation skills over Canada were not significant for the week-4 ECCC and JMA forecasts. The peaks in the correlation skill correspond to the centers of action of the PNA and NAO.

The forecast skill for the PNA phase and amplitude was largely independent of ENSO conditions up to a lead time of 3 weeks. The skill for the PNA phase and amplitude was better for El Niño years than neutral years at a lead time of 4 weeks. Although the skill associated with PNA was also better for La Niña years than neutral years, all of the NWP models showed a negative PNA bias. This tendency appears in the composite of the predicted Z500 anomaly and is expected to adversely affect predictions of surface temperature and precipitation over North America (DelSole et al., 2017; Wang and Robertson, 2019). The position of the exit of the Pacific jet in the predictions would lead to the negative PNA bias seen in La Niña years. The correlation skill and RMSE were higher for the El Niño years than neutral years in the week-2 to -4 forecasts, indicating that the NAO phase and amplitude forecasts are better and worse, respectively, during El Niño years at S2S timescales. The NAO phase predictions were better for the La Niña years than neutral years for lead times up to 4 weeks, but were not as good as those for the El Niño years.

Thus, the PNA and NAO, which are important low-frequency atmospheric variabilities, control sub-seasonal predictability, and this conclusion is in agreement with much previous work (e.g., Lin et al., 2009; Matsueda and Palmer, 2018; Vitart, 2017). ENSO forcing, which is an important coupled atmosphere–ocean process, enhances sub-seasonal predictability by inducing teleconnections. This is consistent with cyclone track predictability at S2S timescales, as found by Zheng et al. (2019). The SST and VP anomaly indicate that a dynamic ocean model has little effect on forecasts of atmospheric response to ENSO forcing in the tropics at S2S timescales. On the other hand, the upper-level jet in mid-latitudes has a more significant influence on the forecast skill of the teleconnections than the atmospheric response in the tropics. Lee et al. (2019) showed that the position of the Pacific and Atlantic jets during different ENSO phases affects the European weather regime associated with MJO phase 3. Therefore, reducing the bias in mid-latitudes would improve the S2S forecasts. This conclusion is consistent with the results of teleconnections associated with the MJO, as reported by Lin (2020). As the ocean state, such as the Kuroshio–Oyashio extension (Zhou and Xie, 2017), influences the variability of the westerly jet in mid-latitudes, further studies are needed to evaluate the effects of atmosphere–ocean coupling in NWP models on S2S predictions.

Acknowledgments

The author thanks to the ECMWF for providing ERA5 and S2S datasets. This study was supported by the Arctic Challenge for Sustainability (ArCS) Project and Japan Society for the Promotion of Science (JSPS) Grant-in-Aid for Research Activity Start-up, Number 19K23454.

References

Brunet, G., Shapiro, M., Hoskins, B., Moncrieff, M., Dole, R., Kiladis, G. N., et al. (2010). Collaboration of the weather and climate communities to advance subseasonal-to-seasonal prediction. *Bulletin of the American Meteorological Society*, 91, 1397–1406. https://doi.org/10.1175/2010BAMS3013.1

DelSole, T., Trenary, L., Tippett, M. K., & Pegion, K. (2017). Predictability of week-3-4 average temperature and precipitation over the contiguous United States. *Journal of Climate*, 30, 3499–3512. https://doi.org/10.1175/JCLI-D-16-0567.1

Hoskins, B. J., & Ambrizzi, T. (1993). Rossby wave propagation on a realistic longitudinally varying flow. *Journal of the Atmospheric Sciences*, 50, 1661–1671. https://doi.org/10.1175/1520-0469(1993)050<1661:RWPOAR>2.0.CO;2

Hoskins, B. J., & Karoly, D. J. (1981). The steady linear response of a spherical atmosphere to thermal and orographic forcing. *Journal of the Atmospheric Sciences*, 38, 1179–1196. https://doi.org/10.1175/1520-0469(1981)038<1179:TSLROA>2.0.CO;2

Hersbach, P., de Rosnay, B., Bell, D., Schepers, A., Simmons, C., Soci, S., et al. (2018). Operational global reanalysis: progress, future directions and synergies with NWP. *ERA report seriese*, https://doi.org/10.21957/tkic6g3wm

Hurrell, J. W. (1995). Decadal trends in the North Atlantic oscillation: Regional temperatures and precipitation. *Science*, 269, 676–679. https://doi.org/10.1126/science.269.5224.676

Lee, R. W., Woolnough, S. J., Charlton-Perez, A. J., & Vitart, F. (2019). ENSO modulation of MJO teleconnections to the North Atlantic and Europe. *Geophysical Research Letters*, 46, 13535–13545. https://doi.org/10.1029/2019GL084683

Lin, H. (2018). Predicting the dominant patterns of subseasonal variability of wintertime surface air temperature in extratropical Northern Hemisphere. *Geophysical Research Letters*, 45, 4381–4389. https://doi.org/10.1029/2018GL077509

Lin, H. (2020). Subseasonal forecast skill over the Northern polar region in boreal winter. *Journal of Climate*, 33, 1935–1951. https://doi.org/10.1175/jcli-d-19-0408.1

Lin, H., Brunet, G., & Derome, J. (2009). An observed connection between the North Atlantic oscillation and the Madden-Julian oscillation. *Journal of Climate*, 22, 364–380. https://doi.org/10.1175/2008JCLI2515.1

Matsueda, M., & Palmer, T. N. (2018). Estimates of flow-dependent predictability of wintertime Euro-Atlantic weather regimes in medium-range forecasts. *Quarterly Journal of the Royal Meteorological Society*, 144, 1012–1027. https://doi.org/10.1002/qj.3265

Quinting, J. F., & Vitart, F. (2019). Representation of synoptic-scale Rossby wave packets and blocking in the S2S prediction project database. *Geophysical Research Letters*, 46, 1070–1078. https://doi.org/10.1029/2018GL081381

Scaife, A. A., Arribas, A., Blockley, E., Brookshaw, A., Clark, R. T., Dunstone, N., et al. (2014). Skillful long-range prediction of European and North American winters. *Geophysical Research Letters*, 41, 2514–2519. https://doi.org/10.1002/2014GL059637

Scaife, A. A., Comer, R. E., Dunstone, N. J., Knight, J. R., Smith, D. M., MacLachlan, C., et al. (2017). Tropical rainfall, Rossby waves and regional winter climate predictions. *Quarterly Journal of the Royal Meteorological Society*, 143(702), 1–11. https://doi.org/10.1002/qj.2910

Soulard, N., Lin, H., & Yu, B. (2019). The changing relationship between ENSO and its extratropical response patterns. *Scientific Reports*, 9. https://doi.org/10.1038/s41598-019-42922-3

Straus, D. M., & Shukla, J. (2000). Distinguishing between the SST-forced variability and internal variability in mid latitudes: Analysis of observations and GCM simulations. *Quarterly Journal of the Royal Meteorological Society*, 126, 2323–2350. https://doi.org/10.1256/smsqj.56715

Straus, D. M., & Shukla, J. (2002). Does ENSO force the PNA? *Journal of Climate*, 15, 2340–2358. https://doi.org/10.1175/1520-0442(2002)015<2340:DEFTP>2.0.CO;2

Toniazzo, T., & Scaife, A. A. (2006). The influence of ENSO on winter North Atlantic climate. *Geophysical Research Letters*, 33, 1–5. https://doi.org/10.1029/2006GL027881

Tseng, K.-C., Barnes, E. A., & Maloney, E. D. (2018). Prediction of the midlatitude response to strong Madden-Julian Oscillation events on S2S time scales. *Geophysical Research Letters*, 45, 463–470. https://doi.org/10.1002/2017GL075734

Vitart, F. (2017). Madden–Julian Oscillation prediction and teleconnections in the S2S database. *Quarterly Journal of the Royal Meteorological Society*, 143, 2210–2220. https://doi.org/10.1002/qj.3079

Vitart, F., Ardilouze, C., Bonet, A., Brookshaw, A., Chen, M., Codorean, C., et al. (2017). The subseasonal to seasonal (S2S) prediction project database. *Bulletin of the American Meteorological Society*, 98, 163–173. https://doi.org/10.1175/BAMS-D-16-0017.1

Walker, G.T., & Bliss, E.W. (1932). World Weather V, *Memoirs of the Royal Meteorological Society*, 4, 53-84.

Wallace, J. M., & Gutzler, D. S. (1981). Teleconnections in the geopotential height field during the Northern Hemisphere winter. *Monthly Weather Review*, 109, 784–812. https://doi.org/10.1175/1520-0493(1981)109<0784:TITGHF>2.0.CO;2

Wang, L., & Robertson, A. W. (2019). Week 3–4 predictability over the United States assessed from two operational ensemble prediction systems. *Climate Dynamics*, 52, 5861–5875. https://doi.org/10.1007/s00382-018-4484-9

White, C. J., Carlsen, H., Robertson, A. W., Klein, R. J. T., Lazo, J. K., Kumar, A., et al. (2017). Potential applications of subseasonal-to-seasonal (S2S) predictions. *Meteorological Applications*, *24*(3), 315–325. https://doi.org/10.1002/met.1654

Yu, B., Lin, H., & Soulard, N. (2019). A comparison of North American surface temperature and temperature extreme anomalies in association with various atmospheric teleconnection patterns. *Atmosphere*, 10, 1–18. https://doi.org/10.3390/atmos10040172

Zampieri, L., Goessling, H. F., & Jung, T. (2018). Bright prospects for Arctic sea ice prediction on subseasonal time scales. *Geophysical Research Letters*, 45, 9731–9738. https://doi.org/10.1029/2018GL079394

Zampieri, L., Goessling, H. F., & Jung, T. (2019). Predictability of Antarctic sea ice edge on subseasonal time scales. *Geophysical Research Letters*, 46, 9719–9727. https://doi.org/10.1029/2019GL084096

Zhang, W., Wang, L., Xiang, B., Qi, L., & He, J. (2015). Impacts of two types of La Niña on the NAO during boreal winter. *Climate Dynamics*, 44, 1351–1366. https://doi.org/10.1007/s00382-014-2155-z

Zhang, W., Wang, Z., Stuecker, M. F., Turner, A. G., Jin, F. F., & Geng, X. (2019). Impact of ENSO longitudinal position on teleconnections to the NAO. *Climate Dynamics*, 52, 257–274. https://doi.org/10.1007/s00382-018-4135-1

Zheng, C., Chang, E. K., Kim, H., Zhang, M., & Wang, W. (2019). Subseasonal to seasonal prediction of wintertime Northern Hemisphere extratropical cyclone activity by S2S and NMME models. *Journal of Geophysical Research: Atmospheres*, 124, 12057–12077. https://doi.org/10.1029/2019JD031252

Zhou, W., & Xie, S. P. (2017). Intermodel spread around the Kuroshio-Oyashio extension region in coupled GCMs caused by meridional variation of the westerly jet from atmospheric GCMs. *Journal of Climate*, 30, 4589–4599. https://doi.org/10.1175/JCLI-D-16-0831.1

Figure 1. Correlation skill for the weekly mean Z500 anomaly at each grid point for the (a) ECCC, (b) ECMWF, (c) JMA, (d) NCEP, and (e) UKMO ensemble mean forecasts for the winters of 1999 to 2010. Hatching indicates correlation skills significant at the 99% confidence level. White circles indicate grid points used in the calculation of the PNA index.

Figure 2. Composite Z500 anomaly calculated from the (a, c) week-3 and (b, d) week-4 forecasts from ECCC, ECMWF, JMA, NCEP, and UKMO and the reanalysis (ERA5; red and blue outlines) during strong (a, b) El Niño and (c, d) La Niña years. The number of samples for each composite is shown in parentheses and the correlation coefficient between composites from each forecast and the reanalysis is shown at upper-right in each panel. The white circles are as in Fig. 1.

Table 1. Correlation skill and RMSE between analyzed and predicted PNA and NAO indices in neutral years (N), and their differences between La Niña and neutral (L–N) years, and El Niño and neutral (E–N) years.

Figure 3. As in Fig. 2, but for SST (red–blue shading) anomaly, velocity potential anomaly at 200 hPa (contours, 5.0×10^5 [m^2/s] interval), and zonal wind at 200 hPa (green hatching indicating ≥25 [m/s]).

Figure 1.

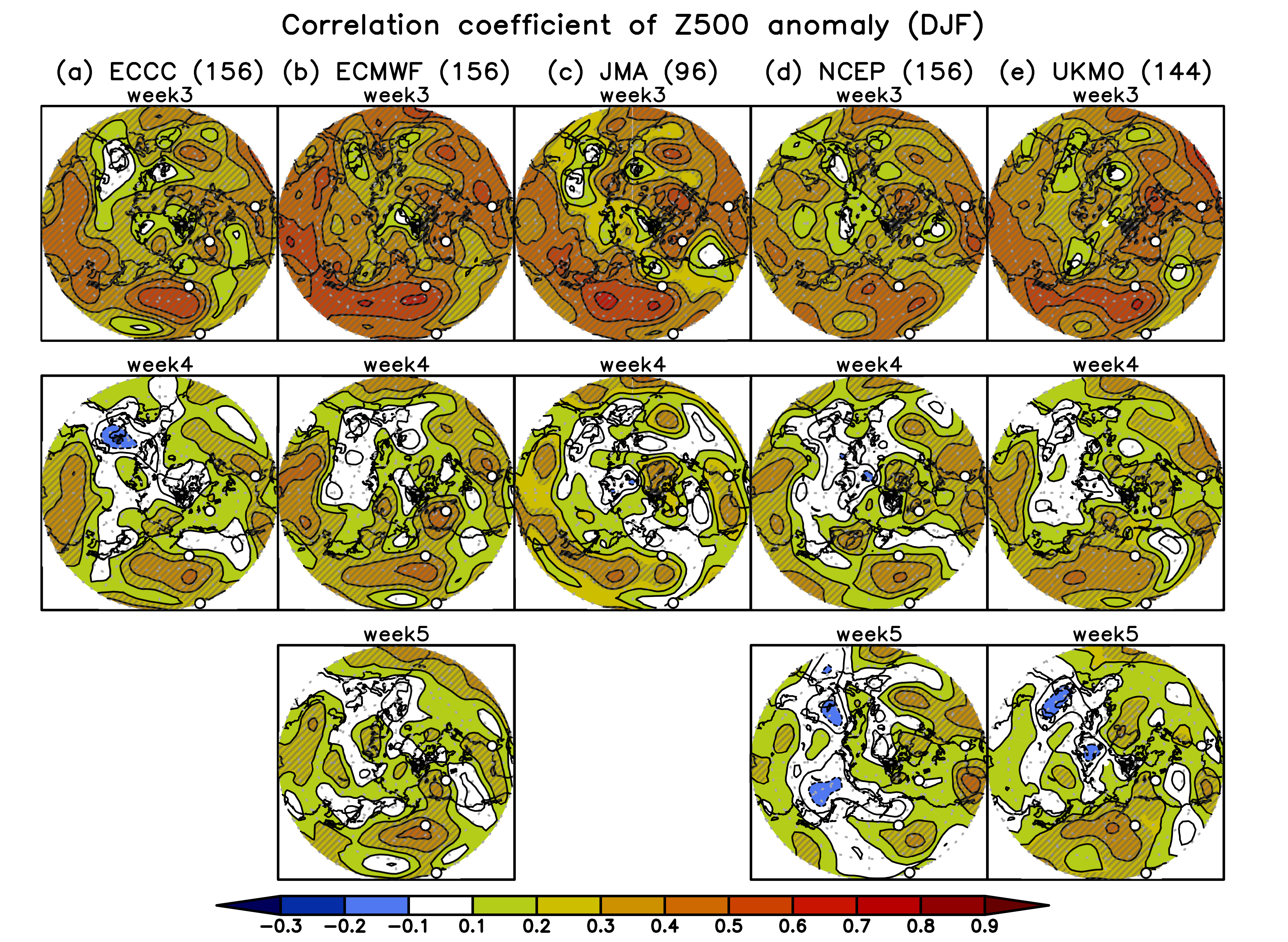
Correlation coefficient of Z500 anomaly (DJF)
(a) ECCC (156)
(b) ECMWF (156)
(c) JMA (96)
(d) NCEP (156)
(e) UKMO (144)
week3
week4
week5
−0.3 −0.2 −0.1 0.1 0.2 0.3 0.4 0.5 0.6 0.7 0.8 0.9

Figure 2.

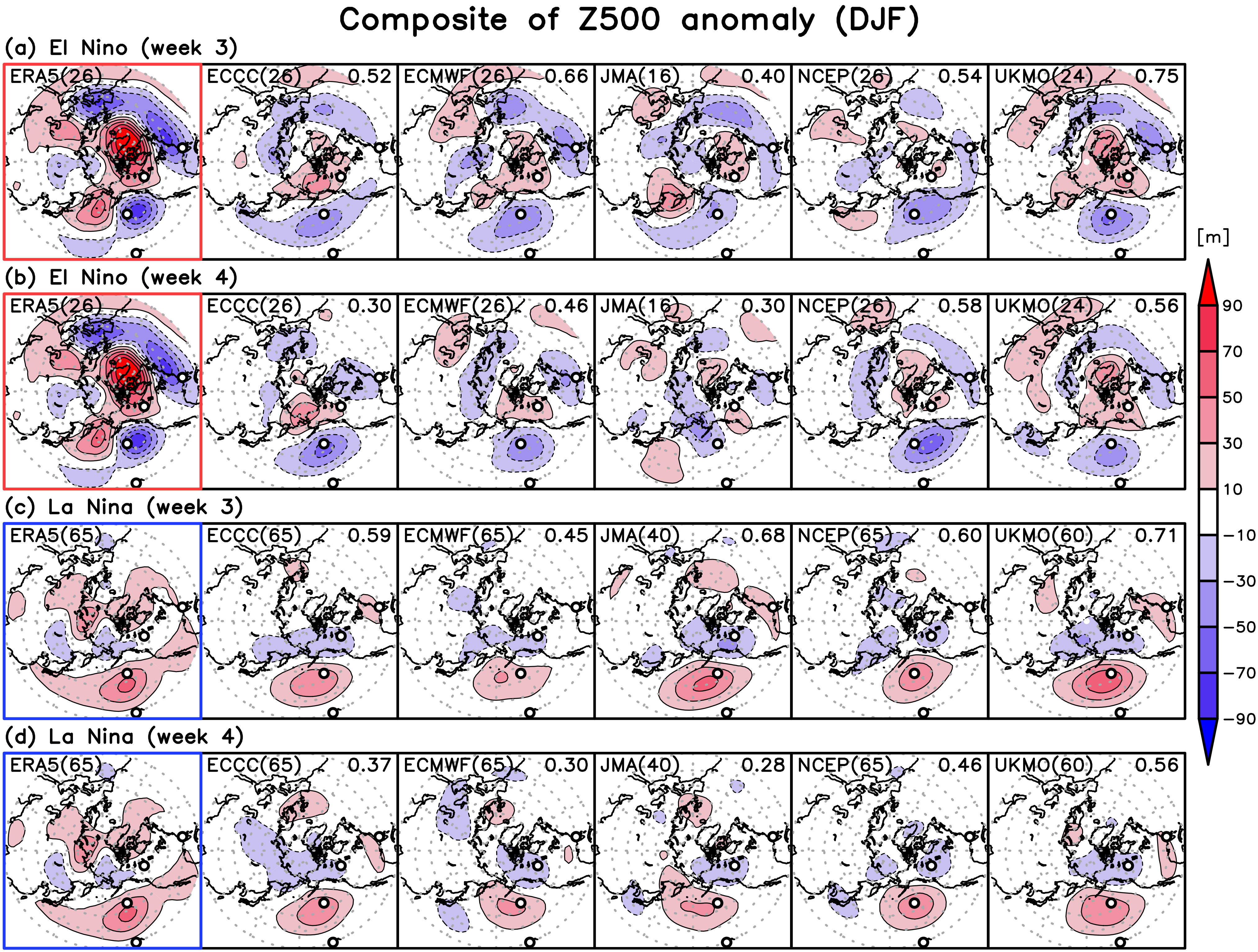
Composite of Z500 anomaly (DJF)
(a) El Nino (week 3)
ERA5(26)
ECCC(26) 0.52
ECMWF(26) 0.66
JMA(16) 0.40
NCEP(26) 0.54
UKMO(24) 0.75
(b) El Nino (week 4)
ERA5(26)
ECCC(26) 0.30
ECMWF(26) 0.46
JMA(16) 0.30
NCEP(26) 0.58
UKMO(24) 0.56
(c) La Nina (week 3)
ERA5(65)
ECCC(65) 0.59
ECMWF(65) 0.45
JMA(40) 0.68
NCEP(65) 0.60
UKMO(60) 0.71
(d) La Nina (week 4)
ERA5(65)
ECCC(65) 0.37
ECMWF(65) 0.30
JMA(40) 0.28
NCEP(65) 0.46
UKMO(60) 0.56
[m]
90
70
50
30
10
−10
−30
−50
−70
−90

			ECCC		ECMWF		JMA		NCEP		UKMO	
			week 3	week 4	week 3	week 4	week 3	week 4	week 3	week 4	week 3	week 4
PNA	Corr. skill	N	0.52	0.20	0.53	0.28	0.39	0.03	0.48	0.20	0.40	0.35
		L–N	-0.01	*0.05*	*0.18*	*0.07*	*0.10*	*0.25*	-0.12	-0.08	*0.07*	-0.13
		E–N	-0.04	*0.30*	*0.12*	*0.12*	-0.01	*0.35*	-0.16	*0.29*	*0.01*	-0.03
	RMSE	N	0.59	0.80	0.65	0.77	0.71	0.85	0.63	0.72	0.63	0.68
		L–N	0.01	*-0.07*	*-0.14*	*-0.06*	*-0.06*	*-0.13*	0.06	0.07	0.04	0.14
		E–N	0.03	*-0.29*	*-0.18*	*-0.11*	*-0.09*	*-0.26*	0.03	*-0.13*	*-0.11*	*-0.09*
NAO	Corr. skill	N	0.28	0.03	0.41	0.01	0.39	0.33	0.37	0.10	0.39	0.11
		L–N	*0.11*	*0.13*	0.00	*0.27*	*0.08*	*0.01*	*0.18*	*0.18*	-0.12	*0.07*
		E–N	*0.30*	*0.20*	*0.29*	*0.56*	*0.17*	*0.10*	*0.08*	*0.41*	*0.15*	*0.59*
	RMSE	N	1.94	2.10	1.71	2.02	1.85	1.83	1.77	2.05	1.78	1.98
		L–N	*-0.08*	0.06	0.07	*-0.11*	*-0.10*	0.11	*-0.13*	*-0.12*	0.24	0.10
		E–N	0.35	0.69	0.39	0.44	0.58	0.94	0.76	0.31	0.34	0.02

Figure 3.

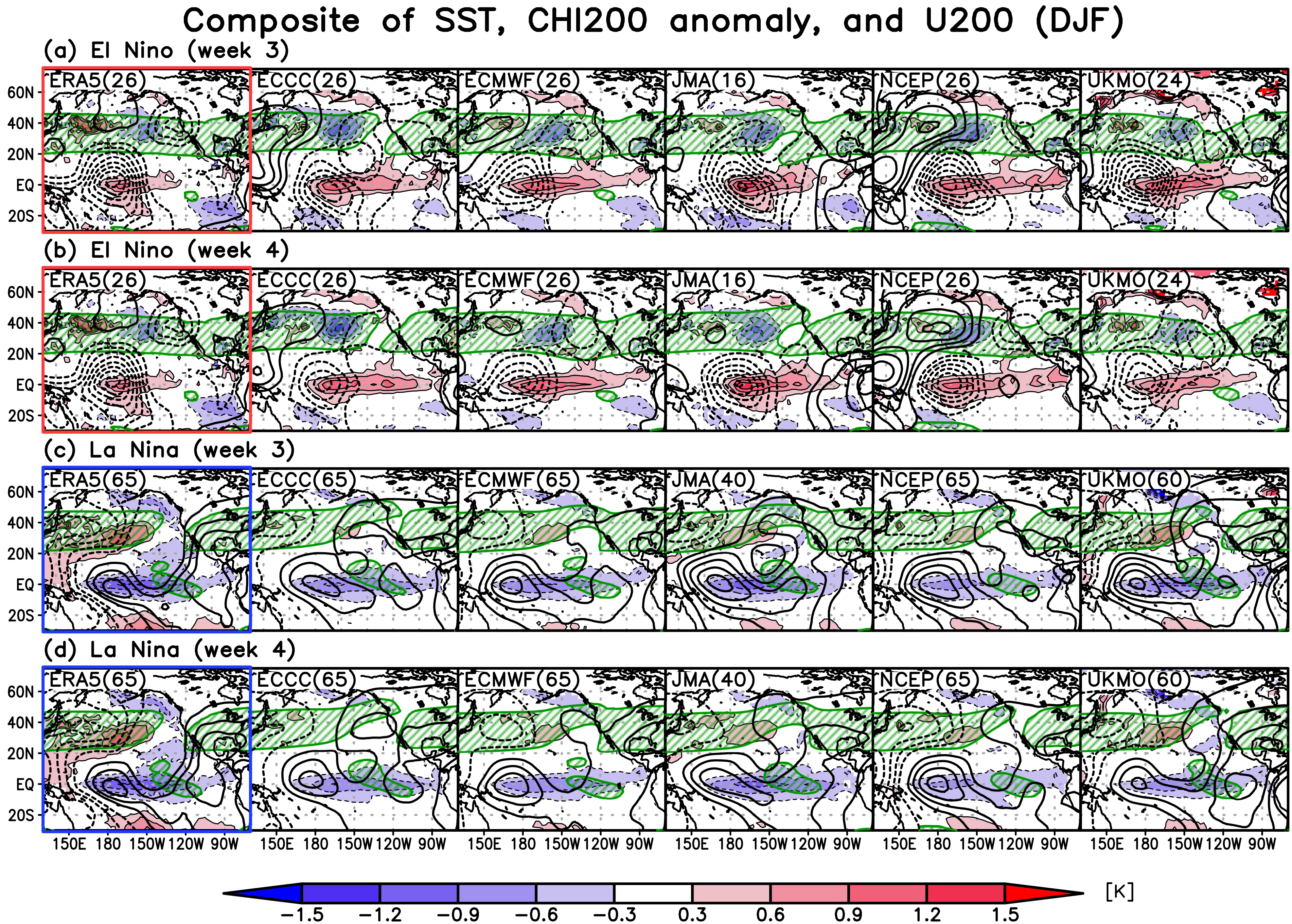

Composite of SST, CHI200 anomaly, and U200 (DJF)
(a) El Nino (week 3)
(b) El Nino (week 4)
(c) La Nina (week 3)
(d) La Nina (week 4)
ERA5(26)
ECCC(26)
ECMWF(26)
JMA(16)
NCEP(26)
UKMO(24)
ERA5(65)
ECCC(65)
ECMWF(65)
JMA(40)
NCEP(65)
UKMO(60)
60N
40N
20N
EQ
20S
150E
180
150W
120W
90W
−1.5
−1.2
−0.9
−0.6
−0.3
0.3
0.6
0.9
1.2
1.5
[K]